

**Supporting Information: Pose Classification using 3D Atomic Structure-
Based Neural Networks Applied to Ion Channel-Ligand Docking**

Heesung Shim^{1*}, Hyojin Kim^{2*}, Jonathan E. Allen³, and Heike Wulff¹

¹ Department of Pharmacology, University of California, Davis, California, 95616, USA

*² Center for Applied Scientific Computing, Lawrence Livermore National Laboratory,
Livermore, California, 94550, USA*

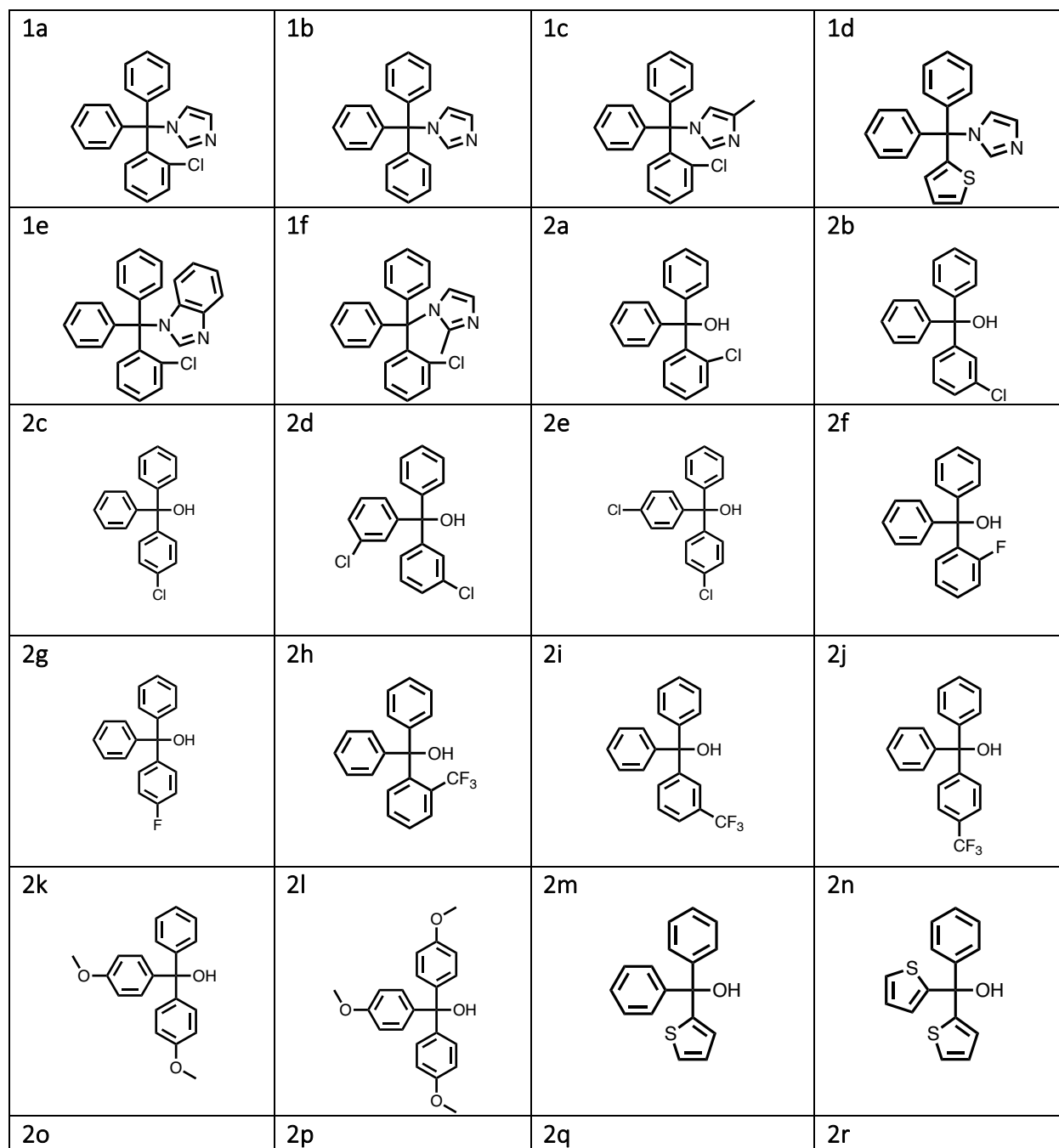
*³ Global Security Computing Applications Division, Lawrence Livermore National
Laboratory, Livermore, California, 94550, USA*

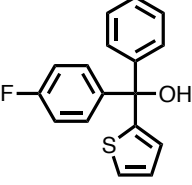
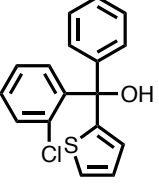
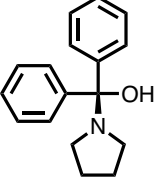
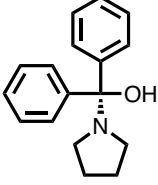
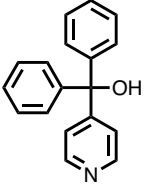
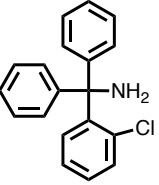
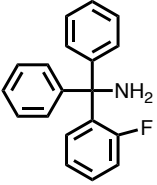
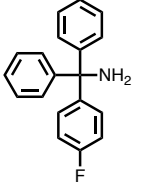
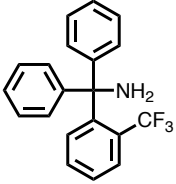
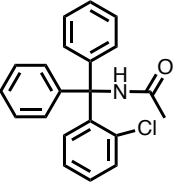
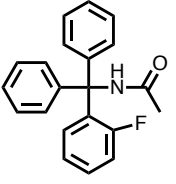
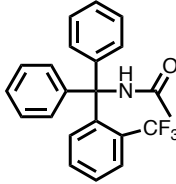
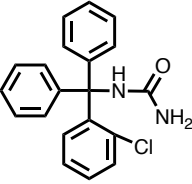
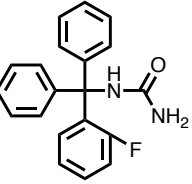
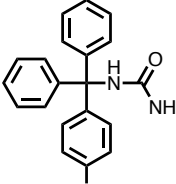
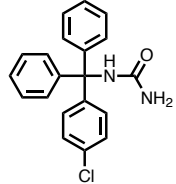
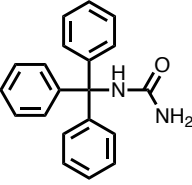
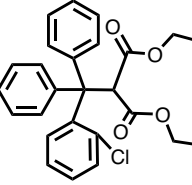
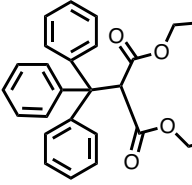
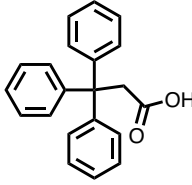
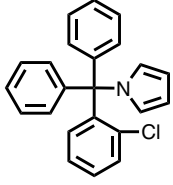
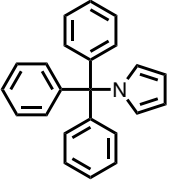
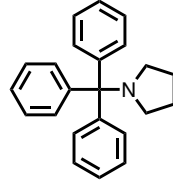
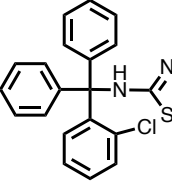
*Corresponding Authors:

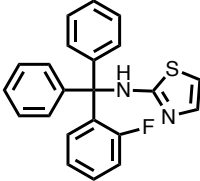
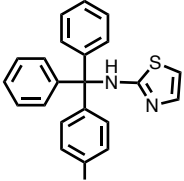
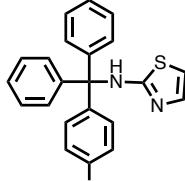
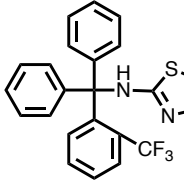
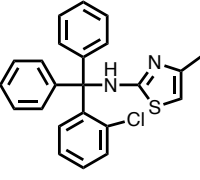
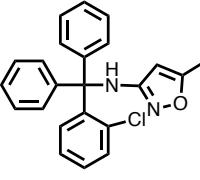
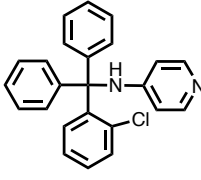
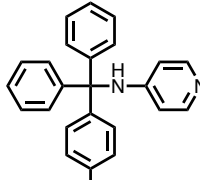
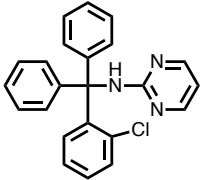
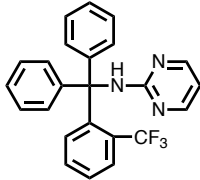
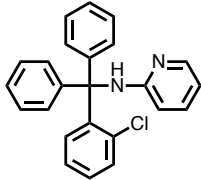
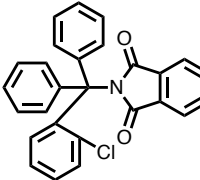
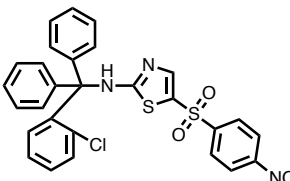
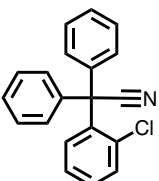
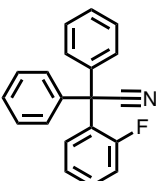
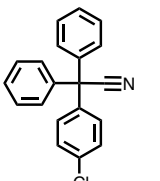
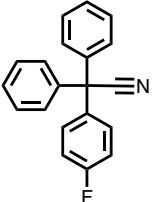
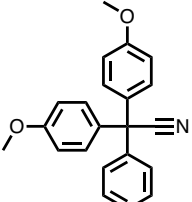
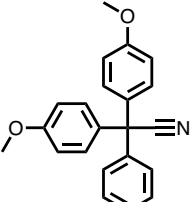
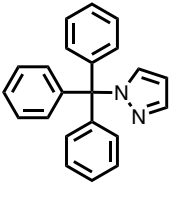
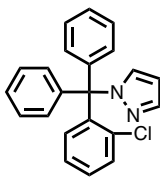
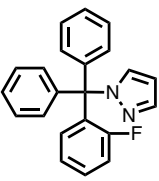
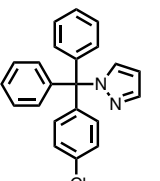
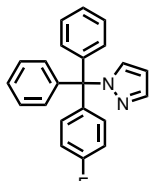
Heesung Shim – hsshim@ucdavis.edu

Hyojin Kim – hkim@llnl.gov

Figure S1 shows all the compound structures of our in-house KCa3.1 inhibitor datasets. Note that the compounds do not have a crystal structure and PDB id.



			
2s	3a	3b	3c
			
3d	3e	3f	3g
			
3h	3i	3j	3k
			
3l	3m	3n	3o
			
4a	4b	4c	4d
			
4e	4f	4g	4h

			
4i	4j	4k	4l
			
4m	4n	4o	4p
			
4q	5a	5b	5c
			
5d	5e	5f	6a
			
6b	6c	6d	6e
			

6f	6g	6h	6i
6j	6k	6l	6m
7a	8a	8b	8c
8d	8e	8f	
N6	R1	R2	R3
R4	R5	R6	R7
R8	R9	S1	S2

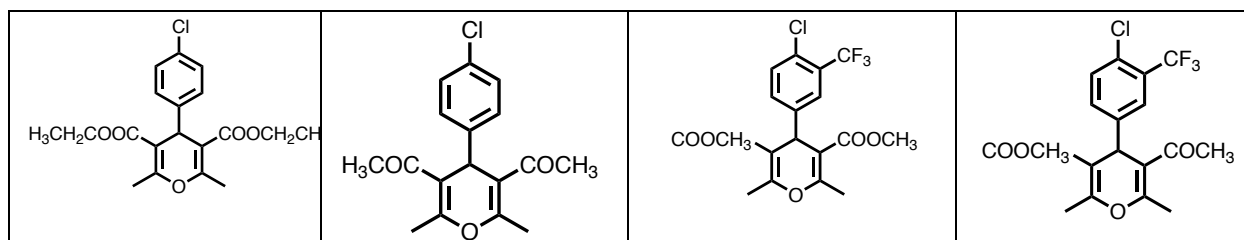
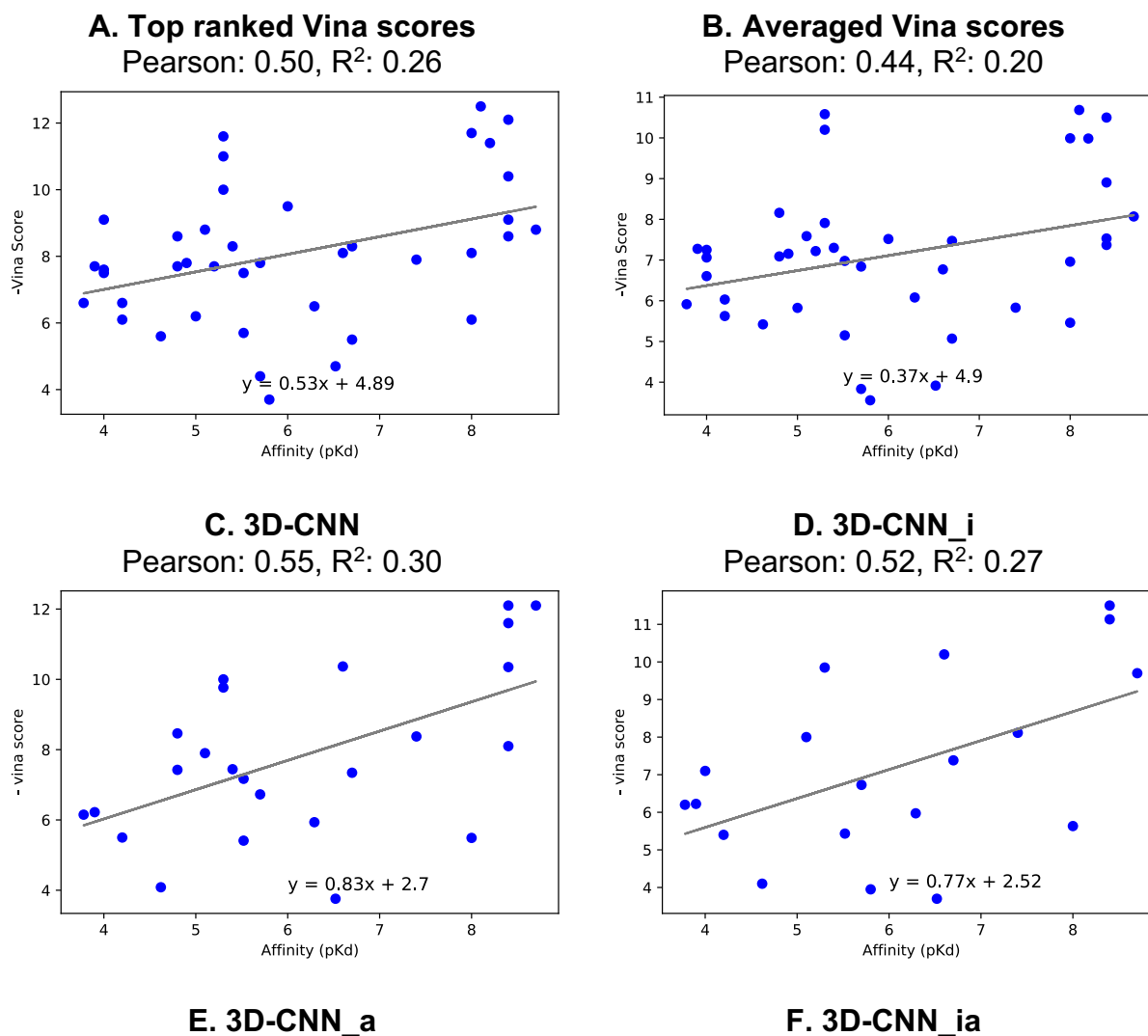


Figure S1: Structures of KCa3.1 channel triarylmethane and cyclohexadiene based inhibitors. Compound 1a-8f were developed by our own group ¹. Compound N6 was developed by NeuroSerach ². Compound R1-S2 were developed by Bayer ^{3, 4}.

Evaluations in subsection 6.3 show the applicability of the proposed pose classifiers filtering out incorrect poses to improve the molecular docking screening. Figure S2 is an extended version of Figure 6 to measure correlations between the Vina docking scores and the binding affinities of the 40 ion channel complexes using all 7 pose classification models. For each model, we measured Pearson and R^2 correlation coefficients with a scatter plot between the Vina scores and the binding affinities.



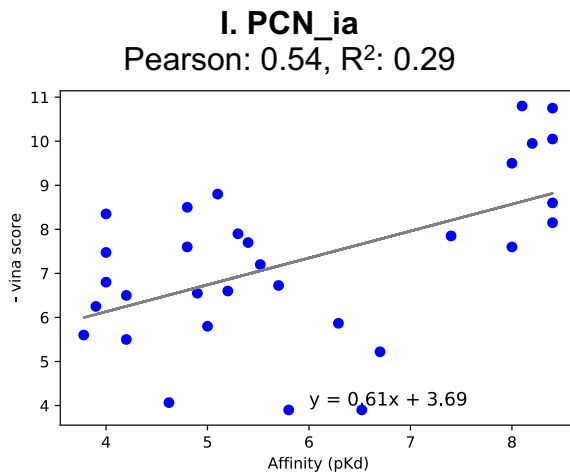
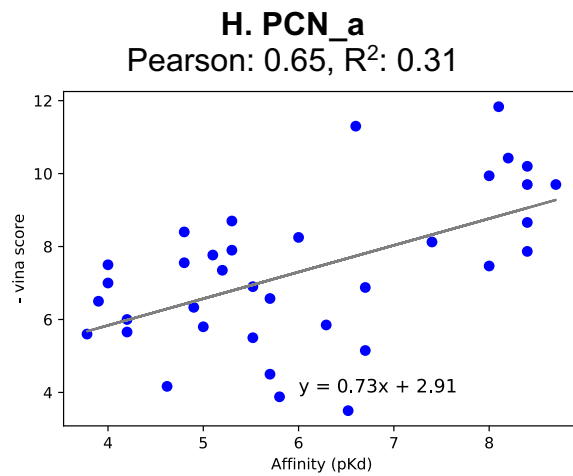
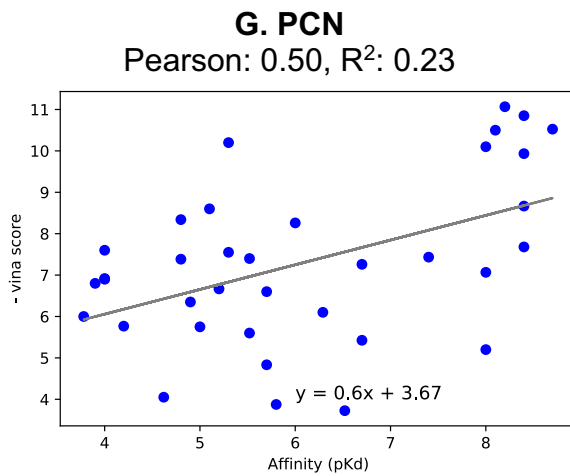
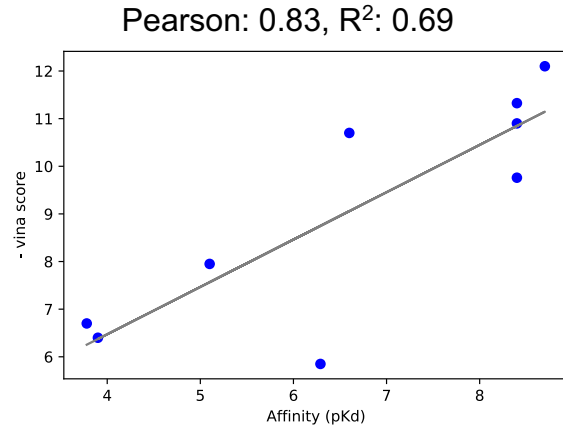
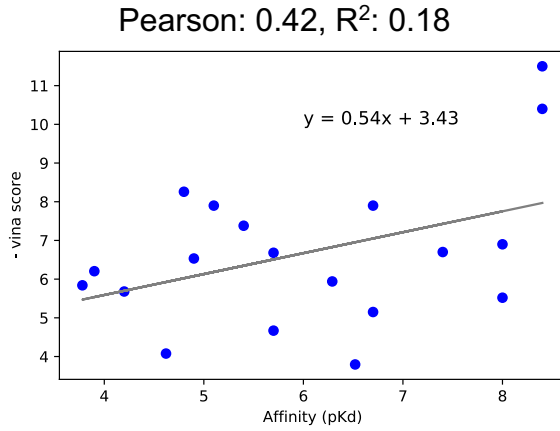
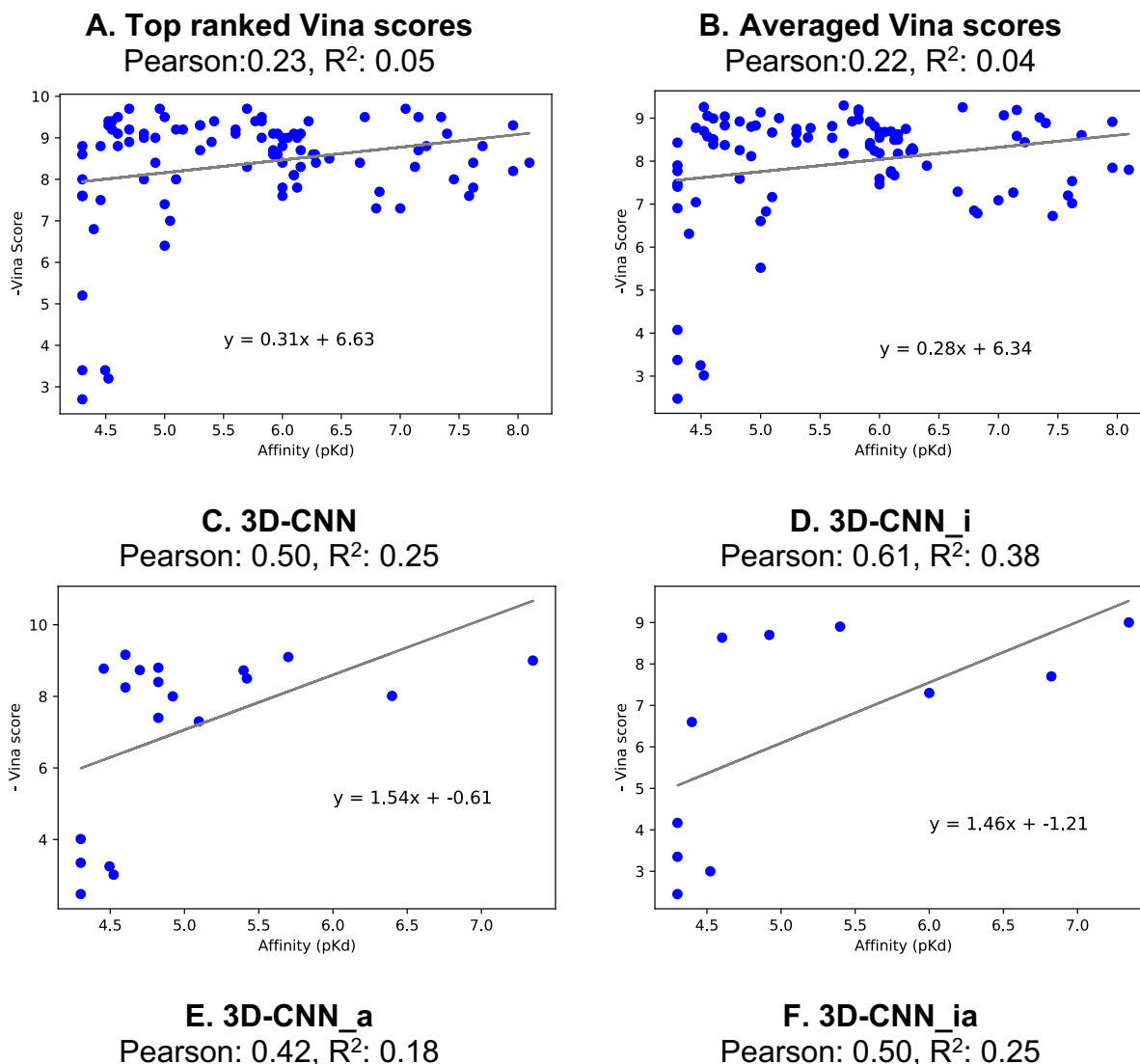
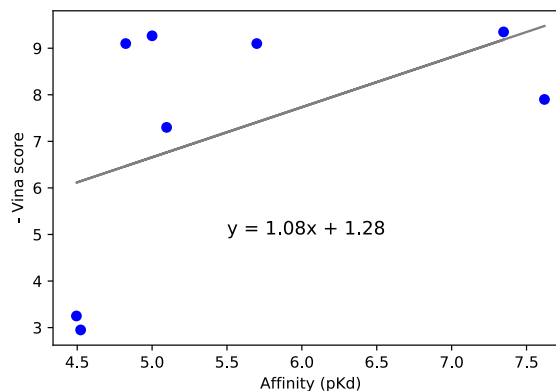
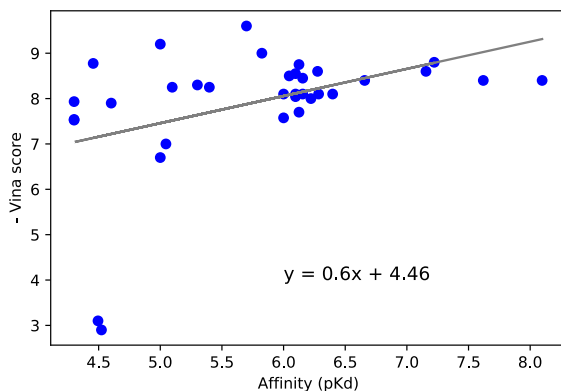


Figure S2: Correlations between the Vina docking scores and binding affinities of the 40 ion channel complexes. A. Top ranked Vina scores; B. Averaged Vina scores; From C to I, Averaged Vina scores across correct poses filtered by 3D-CNN, 3D-CNN with protein-ligand interaction features (3D-CNN_i), 3D-CNN with affine transformation

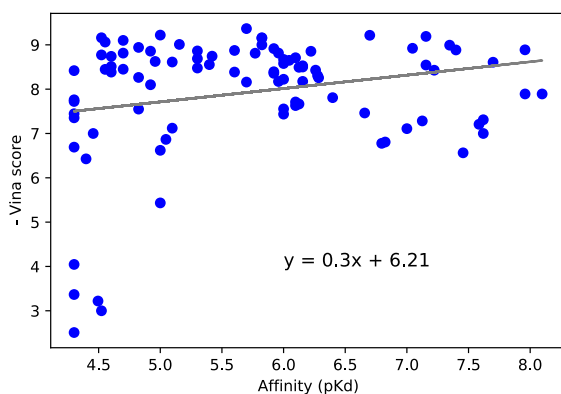
(3D-CNN_a), 3D-CNN with both interaction features and affine transformation (3D-CNN_ia), PCN, PCN with affine transformation (PCN_a), and PCN with both interaction features and affine transformation (PCN_ia), respectively.

Figure S3 and S4 are an extended version of Figure 7 to measure correlations between the docking scores and the binding affinities of the KCa3.1 channel inhibitors complexes using all 7 pose classification models. For each model, we measured Pearson and R^2 correlation coefficients with a scatter plot between the docking scores and the binding affinities. Evaluations shown in Figure S3 and S4 used Vina and Glide docking tools, respectively. Note that Glide is recommended to perform manual preparation of the receptor structure. This tool is not suited to generation of a large number of grids. For that reason, we did not provide a Glide docking evaluation for the 40 ion-channel complex dataset.

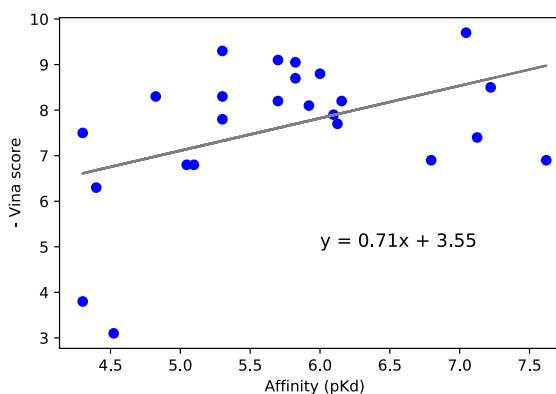




G. PCN
Pearson: 0.23, R^2 : 0.05



H. PCN_a
Pearson: 0.43, R^2 : 0.19



I. PCN_ia
Pearson: 0.46, R^2 : 0.22

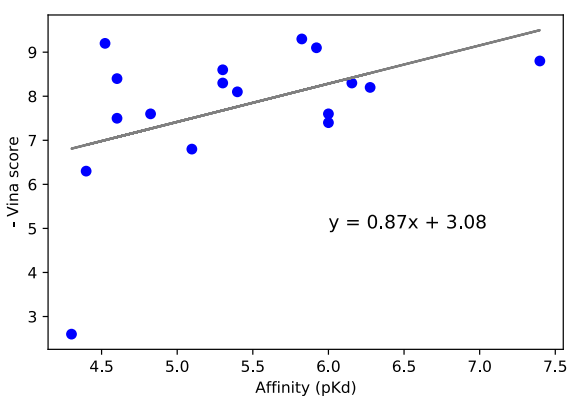
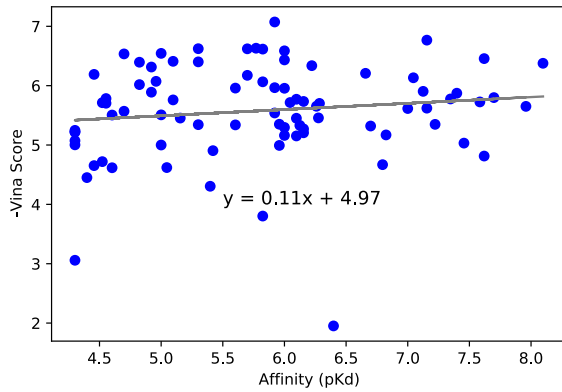


Figure S3: Correlations between the Vina docking scores and binding affinities of the KCa3.1 channel inhibitor complexes. A. Top ranked Vina scores; B. Averaged Vina scores; From C to I, Averaged Vina scores across correct poses filtered by 3D-CNN, 3D-CNN with protein-ligand interaction features (3D-CNN_i), 3D-CNN with affine transformation (3D-CNN_a), 3D-CNN with both interaction features and affine transformation (3D-CNN_ia), PCN, PCN with affine transformation (PCN_a), and PCN with both interaction features and affine transformation (PCN_ia), respectively.

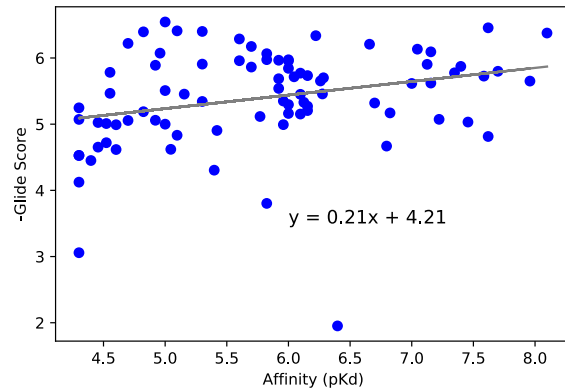
A. Top ranked Glide scores

Pearson: 0.13, R²:



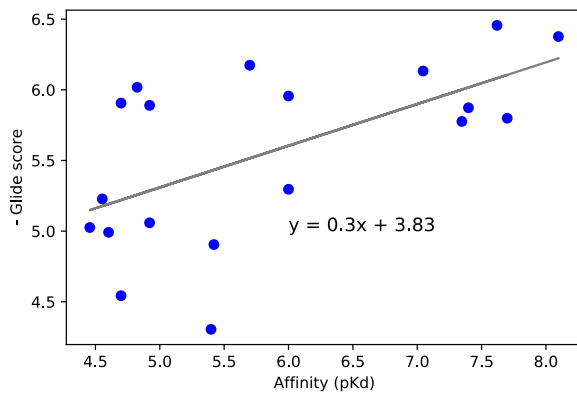
B. Average Glide scores

Pearson: 0.28, R²:



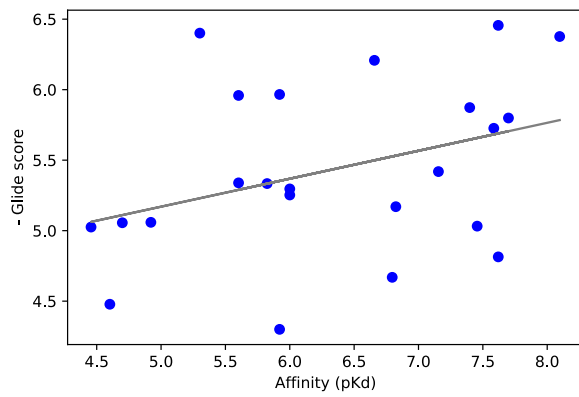
C. 3D-CNN

Pearson: 0.60, R²: 0.35



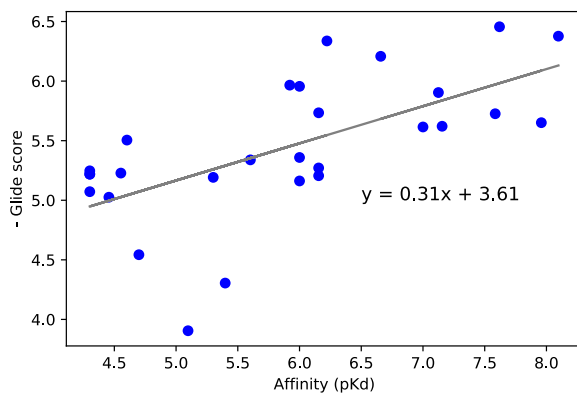
D. 3D-CNN_i

Pearson: 0.36, R²: 0.13



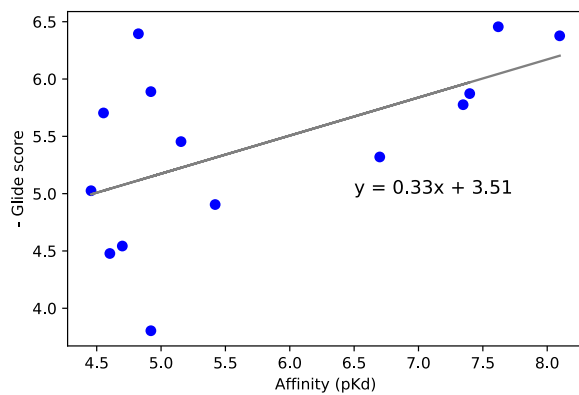
E. 3D-CNN_a

Pearson: 0.63, R²: 0.34



F. 3D-CNN_ia

Pearson: 0.56, R²: 0.31

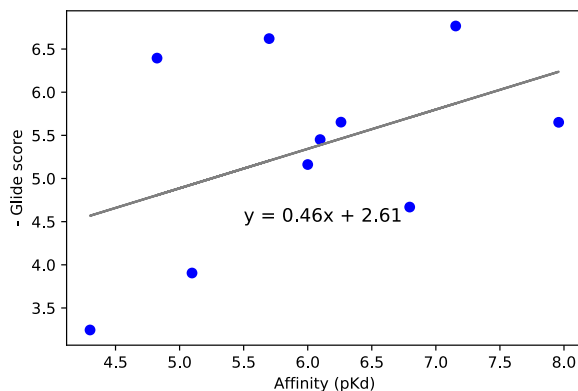
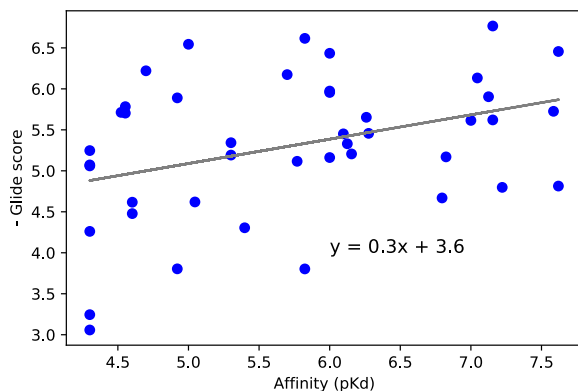


G. PCN

Pearson: 0.37, R²: 0.14

H. PCN_a

Pearson: 0.44, R²: 0.19



I. PCN_ia

Pearson: 0.59, R^2 : 0.35

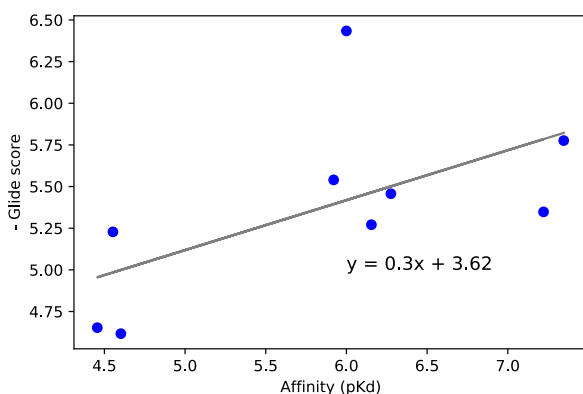


Figure S4: Correlations between the Glide docking scores and binding affinities of the KCa3.1 channel inhibitor complexes. A. Top ranked Glide scores; B. Averaged Glide scores; From C to I, Averaged Glide scores across correct poses filtered by 3D-CNN, 3D-CNN with protein-ligand interaction features (3D-CNN_i), 3D-CNN with affine transformation (3D-CNN_a), 3D-CNN with both interaction features and affine transformation (3D-CNN_ia), PCN, PCN with affine transformation (PCN_a), and PCN with both interaction features and affine transformation (PCN_ia), respectively.

FigureS5 and S6 are an extended version of Figure 9, showing the Pearson correlations between binding affinity and docking scores of the top 10, 20, 30 and 40 ranked compounds based on the confidence scores of our pose classifier models on the KCa3.1 channel inhibitor dataset. Overall, the best poses by our pose classifiers and their docking scores increase the correlation to the binding affinity values. The orange colors indicate with classifier and the blue colors indicate without classifier.

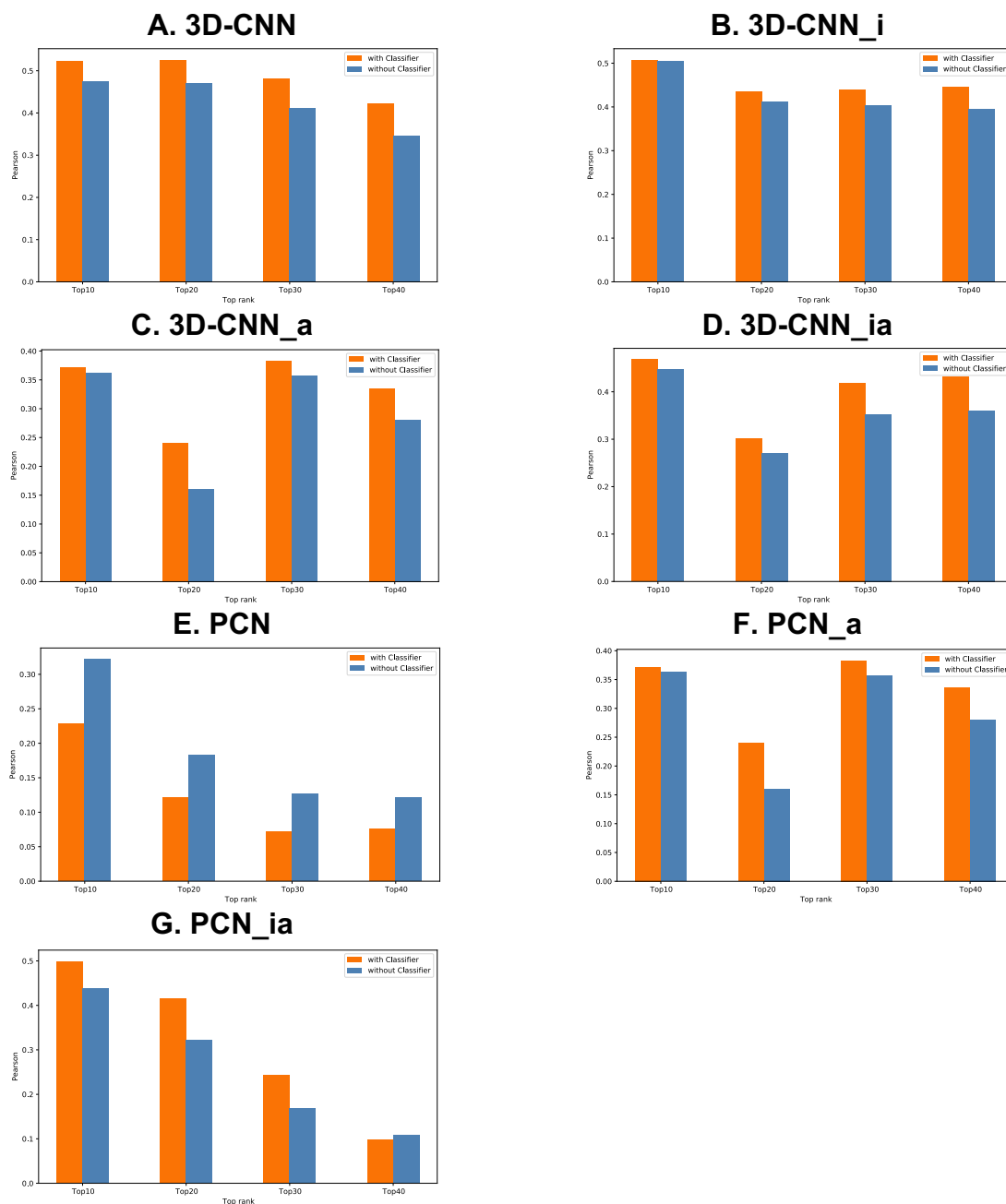


Figure S5: Pearson correlations between binding affinity and docking scores of the Vina top 10, 20, 30 and 40 ranked compounds based on the confidence scores of our pose classifier models on the KCa3.1 channel inhibitor dataset. From A to

G, 3D-CNN, 3D-CNN with protein-ligand interaction features (3D-CNN_i), 3D-CNN with affine transformation (3D-CNN_a), 3D-CNN with both interaction features and affine transformation (3D-CNN_ia), PCN, PCN with affine transformation (PCN_a), and PCN with both interaction features and affine transformation (PCN_ia), respectively.

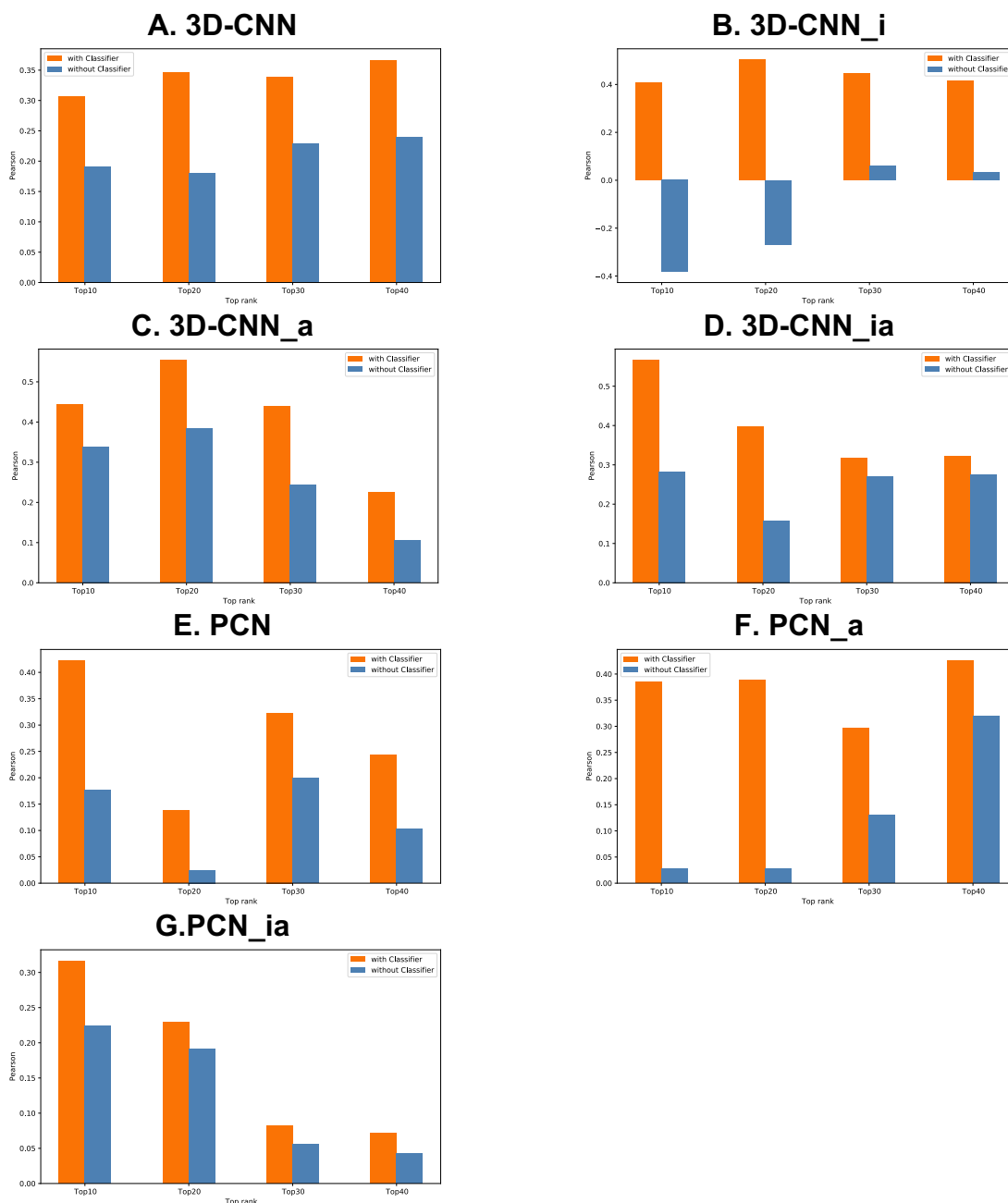


Figure S6: Pearson correlations between binding affinity and docking scores of the Glide top 10, 20, 30 and 40 ranked compounds based on the confidence scores of our pose classifier models on the KCa3.1 channel inhibitor dataset.

From A to G, 3D-CNN, 3D-CNN with protein-ligand interaction features (3D-CNN_i), 3D-CNN with affine transformation (3D-CNN_a), 3D-CNN with both interaction features and affine transformation (3D-CNN_ia), PCN, PCN with affine transformation (PCN_a), and PCN with both interaction features and affine transformation (PCN_ia), respectively.

Figure S7 is an extended version of Figure 10, showing the top 10 ranked compounds in the KCa3.1 channel inhibitor dataset using the 4 best performing pose classifiers (3D-CNN_a, 3D-CNN_ia, PCN_a, PCN_ia). The figure shows that all 4 models yield more strong binders than the one without using any pose classifier.

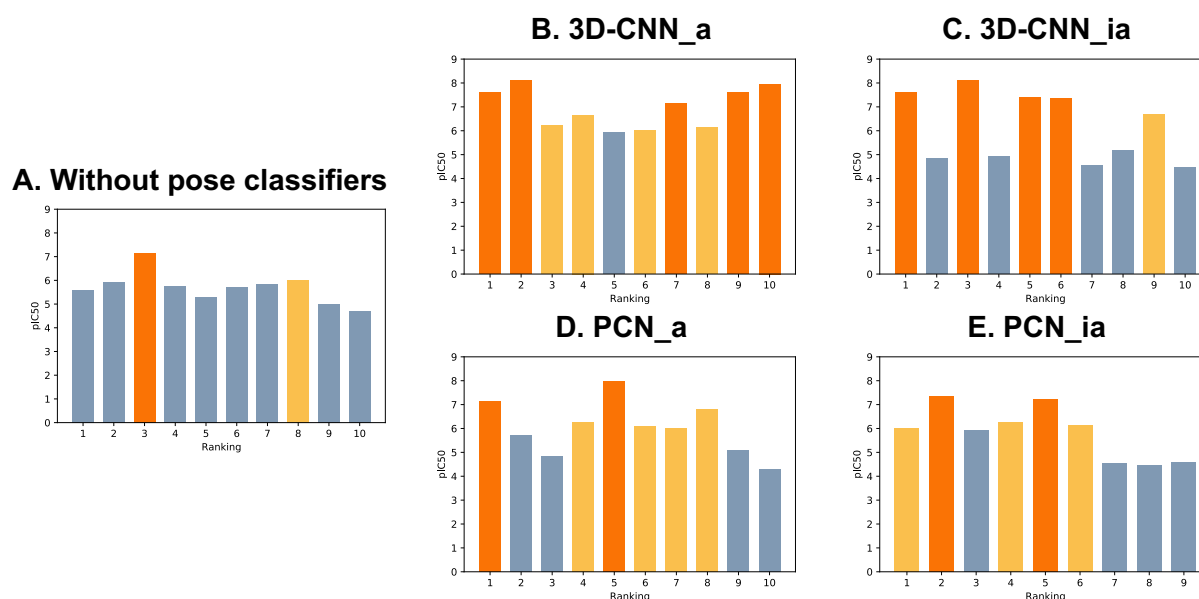


Figure S7: pIC50 of the top 10 ranked compounds in the KCa3.1 channel inhibitor dataset without and with the pose classifiers. A. pIC50 of the top 10 ranked compounds without the pose classifiers. B-E: pIC50 of the top 10 ranked compounds after the pose classifiers are applied (3D-CNN_a, 3D-CNN_ia, PCN_a, PCN_ia, respectively). The orange colors indicate strong binders ($pIC50 \geq 7$). The yellow colors correspond to compounds with $6 \leq pIC50 < 7$. Since PCN_ia classified compound poses aggressively, only 9 compounds were left.

Reference

1. Wulff, H.; Miller, M. J.; Hansel, W.; Grissmer, S.; Cahalan, M. D.; Chandy, K. G., Design of a potent and selective inhibitor of the intermediate-conductance Ca^{2+} -activated K^{+} channel, IKCa1: a potential immunosuppressant. *Proc Natl Acad Sci U S A* **2000**, *97* (14), 8151-6.
2. Strobaek, D.; Brown, D. T.; Jenkins, D. P.; Chen, Y. J.; Coleman, N.; Ando, Y.; Chiu, P.; Jorgensen, S.; Demnitz, J.; Wulff, H.; Christophersen, P., NS6180, a new K(Ca) 3.1 channel inhibitor prevents T-cell activation and inflammation in a rat model of inflammatory bowel disease. *Br J Pharmacol* **2013**, *168* (2), 432-44.
3. Urbahns, K.; Goldmann, S.; Kruger, J.; Horvath, E.; Schuhmacher, J.; Grosser, R.; Hinz, V.; Mauler, F., IKCa-channel blockers. Part 2: discovery of cyclohexadienes. *Bioorg Med Chem Lett* **2005**, *15* (2), 401-4.
4. Urbahns, K.; Horvath, E.; Stasch, J. P.; Mauler, F., 4-Phenyl-4H-pyrans as IK(Ca) channel blockers. *Bioorg Med Chem Lett* **2003**, *13* (16), 2637-9.